v. 4, n. 10, 2024

Journal of Engineering Research

THERMAL EFFICIENCY IN HYDROGEN PRODUCTION: ANALYSING SPIRAL BAFFLED JACKETED REACTORS IN THE CU-CL CYCLE

Mohammed Wassef Abdulrahman
Rochester Institute of Technology

Abstract: This study conducts a heat transfer analysis on a three-phase oxygen reactor equipped with a spiral baffled jacket, assessing the number of reactors needed to achieve various hydrogen production rates through enough heat input. It explores the efficiency of helium gas and molten CuCl in transferring heat from the jacket to the process side of the reactor. Considering a nuclear reactor as the primary heat source for the Cu-Cl cycle, the analysis focuses on two nuclear reactor types: the CANDU Super Critical Water Reactor (CANDU-SCWR) and the High Temperature Gas Reactor (HTGR). Findings indicate that the major thermal resistance in the jacketed oxygen reactor system stems from the reactor wall, contributing approximately 80% to the total thermal resistance due to conduction. The study suggests that the SCWR requires a higher heat transfer rate compared to the HTGR. In terms of fluid choice for the jacket's service side, helium gas is recommended over molten CuCl for better heating efficiency. Furthermore, the analysis concludes that determining the oxygen reactor's size should be based on heat balance calculations, rather than material balance considerations.
Keywords: Cu-Cl cycle; hydrogen production; oxygen; heat transfer; Spiral Baffled Jacket

INTRODUCTION

Hydrogen is increasingly recognized as a key solution to the issue of greenhouse gas emissions, resulted from the global reliance on fossil fuels. Its role in reducing atmospheric pollution and thus decreasing climate change, by limiting greenhouse gas emissions, established hydrogen as a cornerstone for future sustainable energy systems. However, the rapid expand of demand for hydrogen faces some challenges: the need for its sustainable production at scale and at costs competitive with current technologies, without resorting to fossil fuels. In this regard, nuclear energy emerges as a viable option for large-scale, sustainable hydrogen production.

The integration of thermochemical cycles with nuclear reactors presents a viable pathway for the decomposition of water into hydrogen and oxygen via a sequence of intermediate reactions. The copper-chlorine (Cu-Cl) cycle, highlighted by the Argonne National Laboratories (ANL) as a notably efficient low-temperature option (Serban et al., 2004), involves a series of four reactions—three thermal and one electrochemical—highlighting its potential in the sustainable production of hydrogen. The four reaction steps of the Cu-Cl cycle are:

$4CuCl\ (aq) \rightarrow 2CuCl_2\ (aq) + 2Cu\ (s)$, electrolytic process at 25°C step (1)

$2Cu(s) + 2HCl\ (g) \rightarrow 2\ CuCl\ (l) + H_2\ (g)$, hydro-production at 450°C step (2)

$2CuCl_2(s) + H_2O\ (g) \leftrightarrow Cu_2OCl_2(s) + 2HCl\ (g)$, hydrolysis at 375°C step (3)

$Cu_2OCl_2(s) \rightarrow 2CuCl\ (l) + ½\ O_2\ (g)$, thermolysis at 550°C step (4)

During the oxygen production step (step 4), an intermediate compound, solid copper oxychloride (Cu_2OCl_2), is decomposed, yielding oxygen gas and molten cuprous chloride (CuCl). This process is fed by anhydrous solid Cu_2OCl_2, which is obtained from the $CuCl_2$ hydrolysis reaction (step 3), operating at a temperature range of 350-450°C. The outputs from the oxygen reactor are not limited to the desired oxygen gas but may also include potential impurities from side reactions, such as CuCl vapor, chlorine gas, and trace amounts of HCl gas and H_2O vapor. The endothermic reaction of Cu_2OCl_2 decomposition, requiring a reaction heat of 129.2 kJ/mol at a temperature of 530°C, which is the highest temperature point in the Cu-Cl cycle, highlighting the intrinsic thermodynamic difficulties of this procedure (Zamfirescu et al., 2010).

The investigation into the thermochemical properties of copper oxychloride by Ikeda and Kaye (2008) and later by Trevani et al. (2011) provided foundational insights into this compound, which is not commercially available, thus necessitating the development of synthesis methods. These studies are crucial for understanding the behaviour of Cu_2OCl_2 under the conditions present in the Cu-Cl cycle. Lewis et al. (2005) contributed significantly by detailing the experimental status of each reaction within the Cu-Cl cycle, particularly focusing on the evolution of oxygen when Cu_2Cl_2O is subjected to temperatures of 530°C. Their work clarified the oxygen recovery process, a critical component for assessing the cycle's efficiency.

Further exploration of the thermophysical properties of compounds relevant to the Cu-Cl cycle was conducted by Zamfirescu et al. (2010), who not only gathered existing experimental data but also developed new regression formulae to correlate properties such as specific heat, enthalpy, entropy, Gibbs free energy, density, formation enthalpy, and free energy. These properties were evaluated under conditions similar to the operating conditions of the Cu-Cl cycle, providing a comprehensive overview of the material characteristics involved.

The scale-up of oxygen reactor technologies has been a focus of research due to the increasing demand for hydrogen and the need for efficient production methods. Abdulrahman (2013a, 2016a, 2022a) delved into the feasibility of scaling up the oxygen reactor, analyzing the optimum size and number of reactors required to meet different oxygen and hydrogen production rates. His analysis highlighted the factors that significantly influence reactor sizing, such as residence times, hydrogen production rate, and mass and heat transfer rates. Abdulrahman's further studies (2016b, 2013b, 2019a-b, 2022b) on the scale-up analyses from the perspective of indirect heat transfer, utilizing a jacketed reactor, and a helical tube inside the reactor (Abdulrahman, 2016c), emphasized the importance of heat balance over material balance in determining reactor size.

Empirical equations formulated from direct contact heat transfer and hydrodynamics experiments within the oxygen reactor (Abdulrahman, 2015, 2016d-e, 2018, 2020a, 2019c) contributed valuable data for optimizing reactor design and operation. These studies were complemented by Computational Fluid Dynamics (CFD) simulations to examine the hydrodynamics and heat transfer within the oxygen slurry bubble column reactor, employing a 2D and 3D Eulerian-Eulerian approach (Abdulrahman, 2016f-g, 2020b-c, 2022c-d, 2023a-c; Nassar, 2023), offering a detailed view of the flow dynamics and thermal behaviors critical to the reactor's efficiency.

This study analytically explores the heat balance within the Cu-Cl cycle's oxygen reactor, particularly focusing on how different hydrogen production rates impact it when using a spiral baffled jacketed reactor. It delves into the thermal resistance across various sections of the reactor system, assessing their individual contributions to the overall heat balance. Specifically, the investigation targets the Continuous Stirred Tank Reactor (CSTR) model, heated via a spiral baffled jacket, to understand the dynamics of heat distribution. The analysis includes a comparison of two heat source types: the Super Critical Water Reactor (SCWR) and the High Temperature Gas Reactor (HTGR). Additionally, it evaluates the performance of two distinct working fluids in the reactor's service side, helium gas and CuCl molten salt, aiming to determine the most effective fluid for heat transfer in this context.

THERMAL RESISTANCES

The continuous stirred-tank reactor (CSTR) is usually used for multiphase reactions that have fairly high reaction rates. Reactant streams are continuously fed into the vessel, and product streams are withdrawn. In CSTR, heating is achieved by a number of different mechanisms. The most common one involves the use of a jacket surrounding the vessel.

In a realistic continuous situation, where the reactor contents are at constant temperature, but with different service side inlet and outlet temperatures, the heat flow equation can be expressed by:

$$\dot{Q} = U\, A_s\, \Delta T_{lm} \tag{1}$$

where ΔT_{lm} is the log mean temperature difference between the bulk temperature of the reactor contents (cold temperature), T_c, and the temperature in the service side, T_H. Since the inside reactor temperature is assumed constant (T_c=530 °C), there is no effect of heat transfer configuration (parallel or counter flow) in the equation of ΔT_{lm} and can be written as:

$$\Delta T_{lm} = \frac{T_{H_{in}} - T_{H_{out}}}{ln\left(\frac{T_{H_{in}} - T_c}{T_{H_{out}} - T_c}\right)} \tag{2}$$

The methodology of calculations depends on the comparison of thermal resistances of each section in the oxygen reactor with the calculated total thermal resistance of the reactor system (R_t). For a hydrogen production rate of 1 kg/day, the total amount of heat required in the oxygen reactor can be calculated as follows;

$$\dot{Q} = \Delta H_r\, \dot{\xi} + \dot{n} \int_{375}^{530} Cp_{Cu_2OCl_2}\, dT = 870\ \text{W} \tag{3}$$

where ΔH_r = 129.162 kJ/mol, $\dot{\xi}$ = 0.5 kmol/day, $\dot{n}_{Cu_2OCl_2}$ = 0.5 kmol/day, $Cp_{Cu_2OCl_2}$ = 134 J/mol.K (Zamfirescu, 2010). The limits of the integral are from 375°C, which is the temperature of the fed solid, to 530°C, which is the temperature of the decomposition process. For a hydrogen production rate of 100 ton/day, is 50000 kmol/day and $\dot{Q}$ will be 87 MW.

For a high temperature gas reactor (HTGR), the nuclear reactor exit temperature is about 1000°C. The inlet temperature of the heating fluid in the jacket (same as the exit temperature of the intermediate heat exchanger (IHE)) is about 900°C (Natesan, 2006). The exit temperature from the jacket is assumed to be 540°C (because the decomposition temperature is 530°C). For a hydrogen production rate of 100 ton/day and number of reactors *N*, the total thermal resistance of the HTGR can be calculated as follows;

$$R_{HTGR} = \frac{1}{UA_s} = \frac{\Delta T_{lm}}{\dot{Q}} = 1.15 \times 10^{-6}\, N \quad \text{K/W} \tag{4}$$

For CANDU supercritical water reactor (CANDU-SCWR), where the nuclear reactor exit temperature is about 625°C (Chow & Khartabil , 2007; Duffey & Leung, 2010) and the inlet and outlet jacket temperatures are about 600°C and 540°C respectively, the total thermal resistance is R_{SCWR} = 3.55 x 10^{-7} *N* K/W for a hydrogen production rate of 100 ton/day.

HEAT TRANSFER ANALYSIS

The resistance to the heat transfer is a composite of the resistances through the various sections indicated in Fig. 1. Using the classical film theory and heat conduction through composite layers, the total thermal resistance () can be expressed as;

$$\begin{aligned} R_t &= R_P + R_{FP} + R_W + R_S + R_{FS} \\ &= \frac{1}{h_P\, \pi\, D_P\, H_R} + \frac{f_P}{\pi\, D_P\, H_R} + \frac{\ln\left(\frac{D_S}{D_P}\right)}{2\, \pi\, k_w\, H_R} + \frac{1}{h_S\, \pi\, D_S\, H_R} + \frac{f_S}{\pi\, D_S\, H_R} \end{aligned} \tag{5}$$

The largest thermal resistance in Eq. (5) dominates the value of the overall heat transfer coefficient.

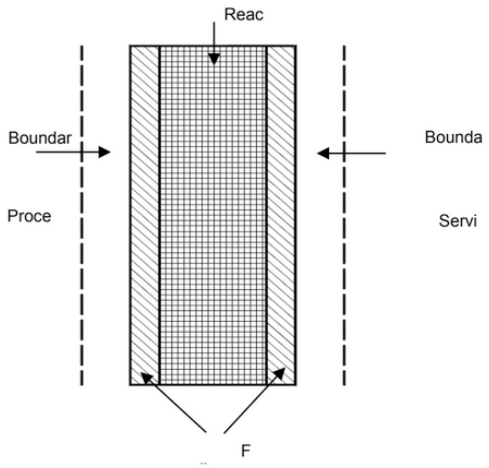

Fig. 1 Thermal resistances through the reactor wall sections.

HEAT TRANSFER THROUGH REACTOR WALL

The stainless steels are the most frequently used corrosion resistant materials in the chemical industry. Types 321, 347 and 348 stainless steels are advantageous for high temperature service (such as in the oxygen reactor) because of their good mechanical properties. They continue to be employed for prolonged service in the 427°C to 816°C temperature range. The physical properties of Types 321, 347 and 348 are quite similar and, for all practical purposes, may be considered to be the same.

The ASME Code provides formulas that relate the wall thickness to the diameter, pressure, allowable stress, and weld efficiency. Since they are theoretically sound only for relatively thin shells, some restrictions are placed on their application. For cylindrical shell under internal pressure, the thickness in inches units is;

$$t = \frac{PR_R}{SE - 0.6P} + t_c \qquad (6)$$

$$conditions: \quad t \le 0.25D_R, \quad P \le 0.385\,SE$$

where T_c is the corrosion allowance in inches, R_R is the outside radius of the cylindrical shell in inches and is the maximum allowable working stress in psi. P is the total pressure which is the sum of the static pressure and operating pressure of the oxygen reactor. The value of the joint efficiency, E, is between 0.6 and 1 (Abdulrahman, 2019b). In order to allow for possible surges in operation, it is customary to raise the maximum operating pressure by 10% or 0.69-1.7 bar over the maximum operation pressure, whichever is greater. The maximum operating pressure in turn may be taken as 1.7 bar greater than the normal (Couper et. al., 2005).

HEAT TRANSFER THROUGH SPIRAL BAFFLED JACKET

The cross section of a spiral baffled jacket is shown in Fig. 2. The spacing between the jacket and reactor wall depends on the size of the reactor, however, it ranges from 50 mm for small reactors to 300 mm for larger reactors. In heat transfer applications, this jacket is considered a special spiral baffling case of a helical coil if certain factors are used for calculating outside film coefficients. The leakage around spiral baffles is considerable, amounting to 35–50% of the total mass flow rate. Due to the extensive leakage, the effective mass flow rate in the jacket is usually taken as 60% of the actual flow rate to get a conservative film coefficient (Coker, 2001).

$$\dot{m}' \approx 0.6\,\dot{m} = 0.6\,\frac{\dot{Q}}{N\,C_p\,(T_{Hout} - T_{Hin})} \qquad (7)$$

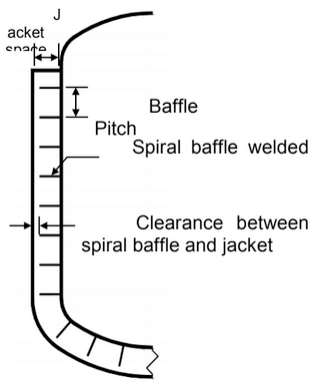

Fig. 2 Cross section of spiral baffled jacket.

where T_{in} and T_{out} are the jacket inlet and outlet temperature respectively. The velocity of the flow in the jacket can be calculated from the effective mass flow rate by;

$$u = \frac{\dot{m}'}{\rho\, A} \tag{8}$$

where A is the spiral baffled jacket cross sectional area and p is the density of the service side fluid (heating fluid). The pitch of the spiral baffled jacket can be calculated from;

$$p = \frac{A}{w} \tag{9}$$

where w is the width of the spiral baffled jacket. The number of coils of the spiral baffled jacket can be calculated from;

$$n = \frac{H_R}{p} \tag{10}$$

where H_R is the height of the reactor. The equivalent heat transfer diameter for the spiral baffled jacket is (Coker, 2001);

$$D_e = 4\, w \tag{11}$$

At a given Reynolds number, heat transfer coefficients of coils, particularly with turbulent flow, are higher than those of long, straight pipes, due to friction. This also applies to flow through a spiral baffled jacket. The equation of heat transfer should be multiplied by a turbulent flow correction factor, involving the equivalent diameter and the diameter of the spiral coil. This correction factor is equal to $\{1 + 3.5(D_e/D_c)\}$, where D_e is the equivalent heat transfer diameter for the spiral baffled jacket, which is calculated from (Coker, 2001): $D_e = 4w$, and D_c is defined as the centerline diameter of the jacket passage.

At Re > 10,000 the Sieder-Tate equation for straight pipe can be used to calculate the outside film coefficient (Coker, 2001);

$$Nu = 0.027\, Re^{0.8}\, Pr^{0.33} \left(\frac{\mu_b}{\mu_w}\right)^{0.14} \left\{1 + 3.5 \left(\frac{D_e}{D_c}\right)\right\} \tag{12}$$

where D_c is defined as the centerline diameter of the jacket passage and is calculated as;

$$D_c = D_{ji} + \frac{D_{j0} - D_{ji}}{2} \tag{13}$$

where D_{ji} and D_{j0} are the inlet and outlet jacket diameter respectively. At Re< 2,100, the following equation can be used (Coker, 2001);

$$Nu = 1.86\, Re^{0.33}\, Pr^{0.33} \left(\frac{\mu_b}{\mu_w}\right)^{0.14} \left(\frac{D_e}{L}\right)^{0.33} \tag{14}$$

where L is the length of the spiral baffled jacket. For 2,100<Re<10,000, above equations can be used depending on the value of Re (Coker, 2001).

PROCESS SIDE HEAT TRANSFER

Oxygen reactor is a multiphase reactor that contains solid particles (Cu_2OCl_2), molten salt (CuCl) and oxygen gas (O_2). In the study of indirect heat transfer, the presence of oxygen gas is neglected, because it is assumed that the oxygen gas will leave the reactor immediately after it is formed. The presence of solid particles will affect the viscosity of the molten salt. Since the density of the Cu_2OCl_2 solid (4080 kg/m^3) has a value near to that of the CuCl molten salt (3692 kg/m^3), it is assumed that solid particles and molten salt are well mixed and form homogeneous slurry. This well mixed homogeneous slurry will lead to a more uniform temperature profile inside the oxygen reactor, that's why the temperature profile is assumed to be constant and equal to 530°C. Thermo physical properties are calculated for the slurry mixture at 530°C.

The dynamic viscosity of slurry can be described as relative to the viscosity of the liquid phase;

$$\mu_{SLR} = \mu_r\, \mu_L \tag{15}$$

where μ_r is the relative dynamic viscosity

(dimensionless), μ_L is the dynamic viscosity of the liquid (CuCl molten salt). Depending on the size and concentration of the solid particles, several models exist to describe the relative viscosity as a function of volume fraction ∅ of solid particles.

$$\emptyset = \frac{V_S}{V_{SLR}} \tag{16}$$

where V_S and V_{SLR} are the volumes of solid particles and slurry respectively. In the case of extremely low concentrations of fine particles, Einstein's equation (Einstein, 1906) may be used;

$$\mu_r = 1 + 2.5\,\emptyset \tag{17}$$

In the case of higher concentrations, a modified equation was proposed by Guth and Simba (1936), which considers interaction between the solid particles;

$$\mu_r = 1 + 2.5\,\emptyset + 14.1\,\emptyset^2 \tag{18}$$

Other thermo physical properties of the slurry mixture can be calculated from the volume percent of the solid and molten salt. For example, the average density of the slurry can be calculated as follows;

$$\rho_{SLR} = \rho_S\,\emptyset_S + \rho_L\,(1 - \emptyset_S) \tag{19}$$

where P_s and P_L are the densities of solid and liquid respectively. The average specific heat of the slurry is;

$$Cp_{SLR} = \frac{\rho_S\,Cp_S\,\emptyset_S + \rho_L\,Cp_L\,(1 - \emptyset_S)}{\rho_{SLR}} \tag{20}$$

where Cp_s and Cp_L are the specific heats of the solid and liquid respectively. A first order estimate of the effective thermal conductivity of a fluid filled porous media can be made by simply accounting for the volume fraction of each substance, giving the resulting relation based on the porosity and the thermal conductivity of each substance (Guth & Simba, 1936). Hence, the effective thermal conductivity of the slurry is calculated from;

$$k_{SLR} = k_S\,\emptyset_S + k_L\,(1 - \emptyset_S) \tag{21}$$

where k_s and k_L are the thermal conductivities of the solid and liquid respectively. For an agitated reactor, the inside film heat transfer coefficient (h_p) can be calculated from the following Nusselt number correlation (Coker, 2001);

$$Nu_D = C Re^a\,Pr^b\left(\frac{\mu}{\mu_w}\right)^c \tag{22}$$

where, C is constant, Re = Reynolds number = $\left(\frac{N_A D_A^2 \rho}{\mu_b}\right)$ and the agitator diameter D_A=D_R/3. The values of constant C, and the indices a,b, and c depend on the type of agitator, the use of baffles, and whether the transfer is to the vessel wall or to coils. An agitator is selected on the basis of material properties and the processing required. The heat transfer forms part of a process operation such as suspending or decomposing solid particles and dispersing the oxygen gas in the molten salt. Several methods for selecting an agitator are available (Kline, 1965; Himmelblau et. al., 2008). Penny (1970) showed one method based on liquid viscosity and vessel volume. According to the Penny's graph and the specifications of oxygen reactor contents and size, the type of the impeller that can be used is a propeller with 420 rpm. For baffled reactor, three blades propeller and transfer to reactor wall, the Nusselt number equation is (Coker, 2001);

$$Nu_D = 0.64 Re^{0.67}\,Pr^{0.33}\left(\frac{\mu_b}{\mu_w}\right)^{0.14} \tag{23}$$

$(Re > 5000)$

FOULING RESISTANCE

An important part of the specification for the oxygen reactor is the assignment of fouling effects. A recommended way to provide an allowance for fouling, is the use of individual fouling resistance values R_{fp} and R_{fs}, for the two sides of the oxygen reactor as used in Eq. (5). R_{fp} is the fouling resistance that occurs on the

internal surface of the reactor (process side) as a result of deposits that accumulate from the reactor contents. R_{fS} is the fouling resistance on the service side of the reactor (like jacket). For helium gas heating fluid, R_{fS} is expected to be negligible since there should be no build-up associated with clean dry helium. Values of the fouling resistances are specified which are intended to reflect the values at the point in time just before the exchanger is to be cleaned. Fouling of heat exchange surfaces can cause a dramatic reduction in the performance of the reactor because of the relatively low thermal conductivity of the fouling material.

There are different approaches to provide an allowance for anticipated fouling in the design of oxygen reactor. In all, the result is to provide added heat transfer surface. This generally means that the reactor is oversized for clean operation and barely adequate for conditions just before it should be cleaned.

TYPE OF WORKING FLUID IN THE SERVICE SIDE OF OXYGEN REACTOR

Two types of fluids are highly recommended as working fluid in the oxygen reactor; CuCl molten salt and high-pressure helium gas (He). Helium gas is recommended amongst the other noble gases because of its chemical inertness and the relatively good transport properties (Rousseau & Van Ravenswaay, 2003; Wang et. al., 2002; Kikstra & Verkooijen, 2000).

There are substantial differences between molten salts and high-pressure helium that must be considered in selecting the working fluid as a heating medium in the oxygen reactor. These key differences are thermal performance, materials compatibility, and safety.

THERMAL PERFORMANCE

The thermo-physical properties for high-pressure helium and CuCl molten salt are summarized in Table 1.

Material	Molten Salt (CuCl) (Zamfirescu, 2010)	Helium (7.5 MPa)	Helium (2 MPa)
$T_{melting}$ (°C)	430	-	-
$T_{boiling}$ (°C)	1490	-	-
P (kg/m³)	3692	3.5	0.939
C_p (kJ/kg.°C)	0.66	5.2	5.2
$P\,C_p$ (kJ/m³.°C)	2450	18.2	4.883
k (W/m.°C)	0.23	0.37	0.3687
$\mu \times 10^5$ (pa.s)	260	4.7	4.7
$\nu \times 10^6$ (m²/s)	0.7	13.4	50
Pr	4.29	0.66	0.6624

Table 1 Comparison of thermo-physical properties of helium and CuCl molten salt at an average temperature of 750°C

From Table 1, it can be seen that the volumetric heat capacity, $p\,C_p$, of molten salt is over two orders of magnitude greater than that of high-pressure helium. The much higher $p\,C_p$ of molten salts, compared to high-pressure helium, has a significant effect upon the relative heat transfer capability. In general, a molten salt loop uses piping of smaller diameters, and less pumping power than those required for high-pressure helium. These differences in pumping power and pipe size reduce the capital cost of the piping system, and allow the arrangement of process equipment to be optimized more easily since process heat can be delivered over larger distances easily. Also, heat transfer coefficients for molten salts are typically greater than those for helium.

MATERIALS

Two primary aspects must be considered in selecting the high-temperature materials and heating fluid used for the oxygen reactor: corrosion and high-temperature mechanical properties (strength, creep, and fabric ability). Clean helium clearly does not have the potential to corrode loop materials, while, molten salts exhibit higher corrosion rates. The potential thermal performance advantages of molten salts suggest that the high-temperature

Nuclear Reactor	Fluid	P (MPa)	$\rho\ (\frac{kg}{m^3})$	$\mu \times 10^{-5}\ (\frac{kg}{m.s})$	$k\ (\frac{W}{m.K})$	Pr	Reference
HTGR (720°C)	Helium	1	0.48	4.6	0.36	0.66	(Petersen, 1970)
SCWR (570°C)	Helium	1	0.48	4.13	0.32	0.66	(Petersen, 1970)
HTGR (720°C)	CuCl	0.1	3692	146	0.19	5	(Zamfirescu, 2010)
SCWR (570°C)	CuCl	0.1	3692	188	0.2	6.11	(Zamfirescu, 2010)

Table 2 Physical properties of helium gas and CuCl molten salt for different mean temperatures

corrosion testing with molten salts should be a priority for the oxygen reactor design.

SAFETY

The copper-chlorine process uses chemicals which are hazardous. The heat transfer fluid in the service side of oxygen reactor provides a stored energy source that can potentially be released rapidly, generating mechanical damage and potentially dispersing flammable or toxic chemicals. For helium gas, the stored energy comes from the high pressure of the gas, and the large volume of gas due to the large duct sizes required for transferring helium with reasonable pressure losses. For molten salts, the stored energy comes from the high temperature and high heat capacity of the liquid. This energy can be released if the molten salt mixes with a volatile liquid (e.g. water), through a well-studied phenomenon typically referred to as a "steam explosion." Molten salts, due to their much lower pumping power and small piping size, permit greater physical separation between the nuclear reactor and the hydrogen production plant. This reduces or eliminates the need for berms or other structures to provide isolation between the reactor and hydrogen plant.

RESULTS AND DISCUSSION

HEAT TRANSFER CALCULATIONS OF THE OXYGEN REACTOR SYSTEM

The physical properties of the heating fluid in the service side of oxygen reactor are calculated at the mean temperature of the fluid, which is for a HTGR is 720°C and for SCWR is 570°C. Table 2 shows the physical properties of both helium and molten salt CuCl for both HTGR and SCWR.

For a helium gas with a pressure of 1 MPa and a temperature range of 570-720°C, the compressibility factor range is 1.001426-1.009594 (Petersen, 1970). This factor varies from unity by less than 1% which means that helium gas can be regarded as an ideal gas. The equation of sound for gases is;

$$c = \sqrt{\gamma RT} \tag{24}$$

where Y is an adiabatic index (Y_{He} = 1.6667) and R is the gas constant (R_{He} =2077 $J/Kg.K$). By using Eq. (24), the theoretical maximum speed of a helium gas (which is 1/3 of speed of sound) for a HTGR (T=720°C) is 618 m/s and for a SCWR (T=570°C) is equal to 570 m/s. In this work, to be more conservative for getting incompressible flow, the operating speed of the helium gas is considered to be 300 m/s in baffled jacket reactor for both HTGR

and SCWR. The operating speed of the CuCl molten salt is assumed to be 3 m/s for baffled jacket. These values are within the range of molten salt nuclear reactors reported (Huntley & Silverman, 1976; Caire & Roure, 2007).

The physical properties of the slurry mixture inside the oxygen reactor (process side) are calculated from Eq. (15) to (21). Table 3 shows the physical properties of both the solid particles and the molten salt inside the oxygen reactor at a temperature of 530°C (Zamfirescu, 2010; Marin, 2012).

	$C_p \frac{J}{Kg.K}$	$k \frac{W}{m.K}$	$\rho \frac{Kg}{m^3}$
Solid Cu_2OCl_2	623.7	0.451	4080
Molten salt CuCl	650.8	0.2	3692

Table 3 Physical properties of Cu_2OCl_2 solid and CuCl molten salt at a temperature of 530°C

HEAT TRANSFER BY JACKETED REACTOR

To calculate the thermal resistance of the reactor wall, it is necessary to know the thickness of this wall. The thickness of the reactor wall (t) is calculated from Eq. (6). The pressure, P in Eq. (6) is the design pressure of the oxygen reactor which is taken here as 1.7 bar greater than the normal total pressure. The normal total pressure is the sum of the operating pressure (P_o) that is equal to 1 bar (14.5 psi) and the static pressure (P_S). Thus the design pressure is;

$$P = P_s + P_o + 1.7\ (bar) = \rho\ g\ H_R + P_o + 1.7\ (bar) \quad (25)$$

where p is the density of the slurry that is calculated from Eq. (19). The size of oxygen reactor has been estimated on the basis of the hydrogen production scale, mass balance, residence time, and aspect ratio, among others. The diameter range of 3-4 m and the aspect ratio of 2 were recommended for an industrial hydrogen production scale of over 100 tons/day (Abdulrahman, 2013a). In this work, the value of the reactor diameter is assumed to be 4 m and the height is 8 m.

The material of the reactor wall is assumed to be stainless steel 321 and the maximum allowable working stress (S) for this stainless steel is 3600 psi at T=649°C (Rozic, 1973). The value of the thermal conductivity (k_w) for stainless steel 321 in the temperature range of 20-500°C is 21.4 W/m.K (Wang et. al., 2002). For known corrosive conditions, the corrosion allowance (t_c) is 8.9 mm (0.35 in.) (Chenoweth, 1990). This value is used for the oxygen reactor because of the relative high corrosion susceptibility of CuCl molten salt. The joint efficiency is taken as 0.8. By substituting the above values into Eq. (6), the thickness of the reactor with a diameter of 4 m and a height of 8 m will be, $t = 2.7\ in = 7\ cm$

In order to calculate the thermal resistance due to fouling in the oxygen reactor, the fouling factor must be known or estimated. According to Tubular Exchanger Manufacturers Association (TEMA), the fouling factor for molten heat transfer salts is equal to 0.000088 m^2 K/W (Chenoweth, 1990). In this work, to be more conservative, twice of this value, 0.000176 m^2 K/W, is used to be the fouling factor for molten salt CuCl.

To calculate the thermal resistance of the jacket side, it is assumed that the thickness of the jacket for spiral baffled jacket is $D_R/15$, where D_R is the reactor diameter. Table 4 shows the values of the numbers of oxygen reactors required for each section of the oxygen reactor for different heating fluids and different nuclear reactors. Figure 3 shows a comparison of the number of reactors required between HTGR and SCWR. This comparison is for each section of the oxygen reactor system with a helium gas at a pressure of 1MPa. From Table 4 and Fig. 3, it can be seen that the maximum number of reactors required comes from the wall of the reactor. This is because of the large

thickness and small conductivity of the wall material. The large diameter requires thick wall to provide enough mechanical stresses and the large height produces high static pressure inside the reactor, which in turn requires more thickness for the wall. It can be seen also that the number of oxygen reactors for SCWR are higher than that for HTGR by more than three times. This is because of the higher temperature difference between the service and process sides in the HTGR. This means that using HTGR is more efficient for producing heat to the oxygen reactor than SCWR. Figure 4 shows the total number of jacketed oxygen reactors with each nuclear reactor for both helium gas and CuCl molten salt. From this figure, it can be seen that there is no big differences between helium gas and molten CuCl in heating the jacketed oxygen reactor.

Fig. 5 shows the comparison of number of oxygen reactors versus the hydrogen production rate between material balance and heat balances for both HTGR and SCWR for a residence time of 0.5 hr and for helium gas service fluid. From Fig. 5, it can be seen that the numbers of reactors calculated from heat balance are 18 times higher than that calculated from material balance for HTGR and 57 times for SCWR. That means the design of oxygen reactor size is controlled mainly by the heat balance.

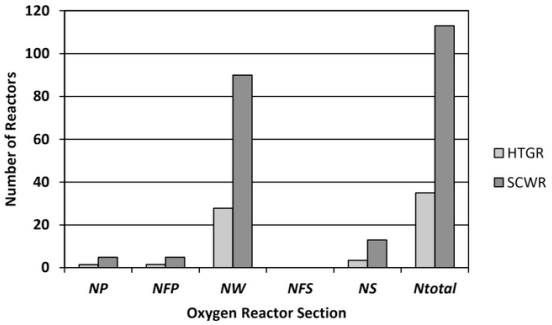

Fig. 3 Number of reactors for each section in oxygen reactor system heated by 1Mpa helium gas for both HTGR and SCWR.

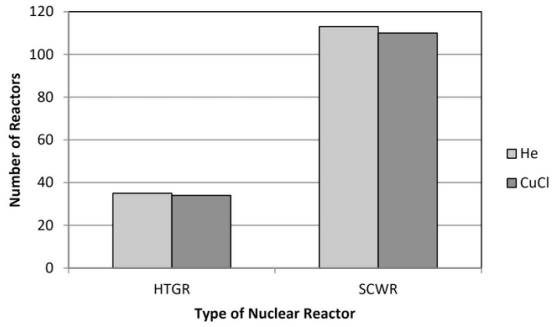

Fig. 4 Total number of oxygen reactors with each nuclear reactor for both 1MPa helium gas and CuCl molten salt.

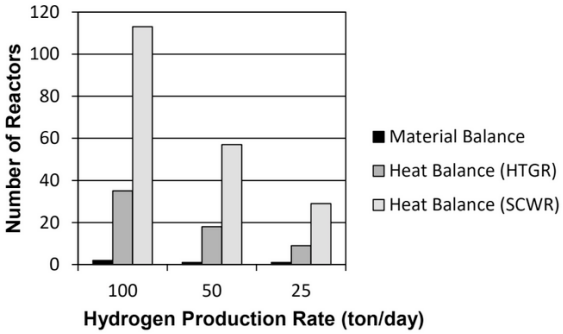

Fig. 5 Number of oxygen reactors calculated by material balance and heat balances of both HTGR and SCWR versus hydrogen production rate for a residence time of 0.5 hr.

CONCLUSIONS

This study establishes that the primary source of thermal resistance in the jacketed oxygen reactor system is the reactor wall, accounting for approximately 80% of the total thermal resistance across both SCWR and HTGR heat sources. The contributions from the service side amount to roughly 10%, while the process side and fouling each add about 4%. The significant thermal resistance of the wall is attributed to its considerable thickness and low thermal conductivity.

Thermal resistance calculations reveal that SCWR requires a lower total thermal resistance compared to HTGR, indicating a need for higher heat transfer rates in SCWR systems. However, HTGR proves more effective than SCWR in facilitating the

Nuclear Reactor Type	Fluid Type	P (MPa)	N_P	NF_P	N_W	N_{FS}	$N_{S\text{-}bafle}$	$N_{total\text{-}baffle}$
HTGR	He	1	1.4	1.5	27.8	0	3.4	35
	CuCl	0.1				1.5	1.4	34
SCWR	He	1	4.9	4.9	90	0	13	113
	CuCl	0.1				4.8	4.6	110

Table 4 Number of reactors of each section of the jacketed oxygen reactor system for different heating fluids and different nuclear reactors

thermal decomposition process within the oxygen reactor, due to a larger temperature differential between the service and process sides in HTGR configurations.

Upon evaluating the thermal efficiency of service side fluids, molten CuCl shows superior thermal performance to helium gas, yet helium gas is favoured over molten CuCl considering material and safety aspects. The analysis finds negligible differences in the required number of reactors when using either fluid, leading to the recommendation of helium gas as the preferred heating medium in the service side of the reactor system.

Moreover, comparing the results derived from material and heat balance assessments, the study concludes that the sizing of the oxygen reactor should be based on heat balance considerations rather than material balance, highlighting the critical role of thermal factors in reactor design and optimization.

REFERENCES

Abdulrahman, M. W. (2015). Experimental studies of direct contact heat transfer in a slurry bubble column at high gas temperature of a helium–water–alumina system. *Applied Thermal Engineering*, *91*, 515-524.

Abdulrahman, M. W. (2016a). *Analysis of the thermal hydraulics of a multiphase oxygen production reactor in the Cu-Cl cycle*. University of Ontario Institute of Technology (Canada).

Abdulrahman, M. W. (2016b). Similitude for thermal scale-up of a multiphase thermolysis reactor in the cu-cl cycle of a hydrogen production. *World Academy of Science, Engineering and Technology, International Journal of Electrical, Computer, Energetic, Electronic and Communication Engineering*, *10*(5), 567-573.

Abdulrahman, M. W. (2016c). Heat transfer analysis of a multiphase oxygen reactor heated by a helical tube in the cu-cl cycle of a hydrogen production. *World Academy of Science, Engineering and Technology, International Journal of Mechanical, Aerospace, Industrial, Mechatronic and Manufacturing Engineering*, *10*(6), 1018-1023.

Abdulrahman, M. W. (2016d). Experimental studies of gas holdup in a slurry bubble column at high gas temperature of a helium– water– alumina system. *Chemical Engineering Research and Design*, *109*, 486-494.

Abdulrahman, M. W. (2016e). Experimental studies of the transition velocity in a slurry bubble column at high gas temperature of a helium–water–alumina system. *Experimental Thermal and Fluid Science*, *74*, 404-410.

Abdulrahman, M. W. (2016f). CFD simulations of direct contact volumetric heat transfer coefficient in a slurry bubble column at a high gas temperature of a helium–water–alumina system. *Applied thermal engineering*, *99*, 224-234.

Abdulrahman, M. W. (2016g). CFD Analysis of Temperature Distributions in a Slurry Bubble Column with Direct Contact Heat Transfer. In *Proceedings of the 3rd International Conference on Fluid Flow, Heat and Mass Transfer (FFHMT'16)*.

Abdulrahman, M. W. (2018). *U.S. Patent No. 10,059,586*. Washington, DC: U.S. Patent and Trademark Office.

Abdulrahman, M. W. (2019a). Heat transfer in a tubular reforming catalyst bed: Analytical modelling. In *proceedings of the 6th International Conference of Fluid Flow, Heat and Mass Transfer*.

Abdulrahman, M. W. (2019b). Exact analytical solution for two-dimensional heat transfer equation through a packed bed reactor. In *Proceedings of the 7th World Congress on Mechanical, Chemical, and Material Engineering*.

Abdulrahman, M. W. (2019c). Simulation of Materials Used in the Multiphase Oxygen Reactor of Hydrogen Production Cu-Cl Cycle. In *Proceedings of the 6 the International Conference of Fluid Flow, Heat and Mass Transfer (FFHMT'19)* (pp. 123-1).

Abdulrahman, M. W. (2020a). *U.S. Patent No. 10,526,201*. Washington, DC: U.S. Patent and Trademark Office.

Abdulrahman, M. W. (2020b). Effect of Solid Particles on Gas Holdup in a Slurry Bubble Column. In *Proceedings of the 6th World Congress on Mechanical, Chemical, and Material Engineering*.

Abdulrahman, M. W. (2020c). CFD Simulations of Gas Holdup in a Bubble Column at High Gas Temperature of a Helium-Water System. In *Proceedings of the 7th World Congress on Mechanical, Chemical, and Material Engineering (MCM'20)* (pp. 169-1).

Abdulrahman, M. W. (2022a). Review of the Thermal Hydraulics of Multi-Phase Oxygen Production Reactor in the Cu-Cl Cycle of Hydrogen Production. In *Proceedings of the 9th International Conference on Fluid Flow, Heat and Mass Transfer (FFHMT'22)*.

Abdulrahman, M. W. (2022b). Heat Transfer Analysis of the Spiral Baffled Jacketed Multiphase Oxygen Reactor in the Hydrogen Production Cu-Cl Cycle. In *Proceedings of the 9th International Conference on Fluid Flow, Heat and Mass Transfer (FFHMT'22)*.

Abdulrahman, M. W. (2022c). Temperature profiles of a direct contact heat transfer in a slurry bubble column. *Chemical Engineering Research and Design*, *182*, 183-193.

Abdulrahman, M. W., & Nassar, N. (2022d). Eulerian Approach to CFD Analysis of a Bubble Column Reactor–A. In *Proceedings of the 8th World Congress on Mechanical, Chemical, and Material Engineering (MCM'22)*.

Abdulrahman, M. W., & Nassar, N. (2023a). A Three-dimensional cfd analyses for the gas holdup in a bubble column reactor. In *Proceedings of the 9th World Congress on Mechanical, Chemical, and Material Engineering (MCM'23)*.

Abdulrahman, M. W., & Nassar, N. (2023b). Three dimensional cfd analyses for the effect of solid concentration on gas holdup in a slurry bubble column. In *Proceedings of the 9th World Congress on Mechanical, Chemical, and Material Engineering (MCM'23)*.

Abdulrahman, M. W., & Nassar, N. (2023c). Effect of static liquid height on gas holdup of a bubble column reactor," In *Proceedings of the 9th World Congress on Mechanical, Chemical, and Material Engineering (MCM'23)*.

Abdulrahman, M. W., Wang, Z., & Naterer, G. F. (2013a). Scale-up analysis of three-phase oxygen reactor in the Cu-Cl thermochemical cycle of hydrogen production. In *EIC Climate Change Technology Conference*.

Abdulrahman, M. W., Wang, Z., Naterer, G. F., & Agelin-Chaab, M. (2013b). Thermohydraulics of a thermolysis reactor and heat exchangers in the Cu-Cl cycle of nuclear hydrogen production. In *Proceedings of the 5th World Hydrogen Technologies Convention*.

Boomsma, K., & Poulikakos, D. (2001). On the effective thermal conductivity of a three-dimensionally structured fluid-saturated metal foam. *International journal of heat and mass transfer*, *44*(4), 827-836.

Caire, J. P., & Roure, A. (2007). Pre design of a molten salt thorium reactor loop.

Chenoweth, J. M. (1990). Final report of the HTRI/TEMA joint committee to review the fouling section of the TEMA standards. *Heat Transfer Engineering*, *11*(1), 73-107.

Chow, C. K., & Khartabil, H. F. (2008). Conceptual fuel channel designs for CANDU-SCWR. *Nuclear Engineering and Technology*, *40*(2), 139-146.

Coker, A. K. (2001). *Modeling of chemical kinetics and reactor design*. Gulf Professional Publishing.

Couper, J. R. (2005). *Chemical process equipment: selection and design*. Gulf professional publishing.

Duffey, R. B., & Leung, L. (2010). Advanced cycle efficiency: generating 40% more power from the nuclear fuel.

Einstein, A. (1906). A new determination of molecular dimensions. *Annln., Phys.*, *19*, 289-306.

Guth, E., & Simba, H. (1936). Viscosity of suspensions and solutions: III Viscosity of sphere suspensions. *Kolloid-Zeitschrift*, *74*, 266-275.

Himmelblau, D. M., Bisio, A., & Kabel, R. L. (2008). *Scaleup of chemical processes*. John Wiley & Sons.

Huntley, W. R., & Silverman, M. D. (1976). *System design description of forced-convection molten-salt corrosion loops MSR-FCL-3 and MSR-FCL-4* (No. ORNL/TM--5540). Oak Ridge National Lab.

Ikeda, B. M., & Kaye, M. H. (2008, August). Thermodynamic properties in the Cu-Cl-OH system. In *7th International conference on nuclear and radiochemistry, Budapest, Hungary*.

Kikstra, J. F., & Verkooijen, A. H. M. (2000). Conceptual design for the energy conversion system of a nuclear gas turbine cogeneration plant. *Proceedings of the Institution of Mechanical Engineers, Part A: Journal of Power and Energy*, *214*(5), 401-411.

Kline, S. J. (1965). *Similitude and approximation theory*. New York, McGraw-Hill.

Lewis, A., Masin, J. G. & Vilim, R. B. (2005). Development of the low temperature cu-cl thermochemical cycle. in *Proceedings of the International Congress on Advances in Nuclear Power Plants*, Argonne National Laboratory, Seoul, Korea.

Marin, G. D. (2012). *Kinetics and Transport Phenomena in the Chemical Decomposition of Copper Oxychloride in the Thermochemical Copper Chloride Cycle*. University of Ontario Institute of Technology (Canada).

Nassar, N. I. (2023). *A Three-Dimensional CFD Analyses for the Hydrodynamics of the Direct Contact Heat Transfer in the Oxygen Production Slurry Bubble Column Reactor of the Cu-Cl Cycle of Hydrogen Production*. Rochester Institute of Technology.

Natesan, K., Moisseytsev, A., & Majumdar, S. (2009). Preliminary issues associated with the next generation nuclear plant intermediate heat exchanger design. *Journal of nuclear materials*, *392*(2), 307-315.

Penny, W. R. (1970). Guide to trouble free mixers. *Chem. Eng.*, vol. 77, no. 12, p. 171.

Petersen, H. (1970). *The properties of helium: density, specific heats, viscosity, and thermal conductivity at pressures from 1 to 100 bar and from room temperature to about 1800 K*. Copenhagen: Jul. Gjellerup.

Rousseau, P. G., & Van Ravenswaay, J. P. (2003, May). Thermal-fluid comparison of three-and single-shaft closed loop brayton cycle configurations for htgr power conversion. In *Proceedings of International Congress on Advances in Nuclear Power Plants (ICAPP'03)*.

Rozic, E. J. (1973). *Elevated temperature properties as influenced by nitrogen additions to types 304 and 316 austenitic stainless steels*. ASTM International.

Serban, M., Lewis, M. A., & Basco, J. K. (2004). *Kinetic study of the hydrogen and oxygen production reactions in the copper-chloride thermochemical cycle*. American Institute of Chemical Engineers.

Trevani, L. (2011, May). The copper-chloride cycle: synthesis and characterization of copper oxychloride. In *Hydrogen and Fuel Cells International Conference and Exhibition*.

Wang, C., Ballinger, R. G., Stahle, P. W., Demetri, E., & Koronowski, M. (2002). Design of a power conversion system for an indirect cycle, helium cooled pebble bed reactor system.

Zamfirescu, C., Dincer, I., & Naterer, G. F. (2010). Thermophysical properties of copper compounds in copper–chlorine thermochemical water splitting cycles. *International Journal of Hydrogen Energy*, *35*(10), 4839-4852.